Biointerface Research in Applied Chemistry
Open-Access Journal (ISSN: 2069-5837)

Article
Volume 16, Issue 3, 2026, 92
https://doi.org/10.33263/BRIAC163.092

Incorporation of Colostrum-derived SIgA into Microemulsions: Stability, Rheology, and Immune Effects

Viviane Francelina Luz [1], Kenia Maria Rezende Silva [2], Nara Cristina Souza Araújo [2], Aron Carlos de Melo Cotrim [1], Eduardo Luzía França [1,2], Adenilda Cristina Honorio França [1,2,*]

[1] Postgraduate Program in Materials Science, Federal University of Mato Grosso, Barra do Garças, MT, Brazil
[2] Institute of Biological and Health Sciences, Federal University of Mato Grosso, Barra do Garças, MT, Brazil
* Correspondence: adenilda.franca@ufmt.br;

Received: 30.11.2025; Accepted: 6.05.2026; Published: 15.06.2026

Abstract: This study investigated the incorporation of colostrum-derived secretory immunoglobulin A (SIgA-C) into oil-in-water (O/W) microemulsions, focusing on physicochemical properties, short-term stability, and *in vitro* immunomodulatory effects. SIgA-C was extracted and standardized to 100 ng·mL^{-1} before incorporation into a microemulsion system composed of surfactants, oil, and aqueous phases. Colostrum-derived SIgA-loaded microemulsion (ME+SIgA-C) displayed Newtonian flow behavior, an acidic pH of 3.93, and electrical conductivity typical of O/W systems. After 15 days of storage, ME+SIgA-C remained homogeneous and translucent, maintaining stability, especially at room temperature (25 ± 2°C). Rheological analysis revealed a statistically significant increase in viscosity over time; however, this variation was minimal and did not affect the flow profile. In oxidative metabolism assays, colostral phagocytes exposed to ME+SIgA-C showed increased superoxide production compared to the control group. At the same time, we observed reduced superoxide dismutase levels and a decrease in the superoxide dismutase/superoxide anion ratio, indicating modulation of the cellular redox balance. These findings demonstrate that SIgA-C can be successfully incorporated into microemulsion systems, which preserve short-term physicochemical stability and maintain immunoreactivity *in vitro*. Further studies, including long-term stability assessments and *in vivo* investigations, are necessary to explore potential biomedical applications.

Keywords: secretory immunoglobulin A; microemulsions; physicochemical properties; stability; immunomodulatory activity.

1. Introduction

Modified drug delivery systems represent an innovative approach for enhancing therapeutic efficacy [1]. Compared to conventional methods, these systems can improve drug bioavailability, enable controlled release, and reduce adverse effects [2,3].

Among these, microemulsions have attracted attention for their thermodynamic stability, isotropy, and ability to solubilize both hydrophilic and lipophilic compounds. Typically composed of oil, water, a surfactant, and sometimes a co-surfactant, microemulsions form nanoscale droplets (<140 nm) that range from translucent to milky white depending on formulation parameters [4,5]. These properties make them suitable carriers for biologically active molecules, including proteins, peptides, and antibiotics [6].

The selection of surfactants and co-surfactants in microemulsion formulations is based on their physicochemical properties [6]. The combination of hydrophobic and hydrophilic surfactants allows achieving a hydrophilic-lipophilic balance compatible with the oil phase, promoting thermodynamically stable systems [7,8]. Non-ionic surfactants, such as sorbitan oleate (SPAN) and polysorbate (TWEEN), are widely used in oral pharmaceutical and food formulations due to their ability to reduce interfacial tension and facilitate the formation of stable droplets without relevant toxicity. Co-surfactants, such as 1-butanol, are frequently employed to increase the flexibility of the interfacial film and to assist in further reducing interfacial tension [4,9-12].

The selection of the Span/Tween/butanol system was based on its ability to achieve an appropriate hydrophilic–lipophilic balance to form stable oil-in-water microemulsions while minimizing protein destabilization. Non-ionic surfactants are preferentially selected due to their lower tendency to induce protein denaturation compared to ionic systems. The inclusion of butanol as a co-surfactant contributes to interfacial flexibility, facilitating the formation of nanoscale droplets and potentially reducing interfacial stress on incorporated biomolecules. Previous studies from our research group using similar microemulsion systems incorporating bioactive molecules, including cytokines and melatonin, did not demonstrate significant alterations in molecular stability or biological activity [7,13,14]. These findings support the preservation of the functional integrity of sensitive biomolecules within this system and reinforce its suitability for the incorporation of secretory immunoglobulin A (SIgA).

Microemulsion systems can exhibit acidic pH, which warrants attention for potential protein denaturation. Changes in the drug microenvironment, such as temperature, hydration state, exposure to organic solvents, pH, or the presence of enzymes, can structurally alter peptides and proteins, potentially rendering them irreversibly inactivated [8,15], which is particularly relevant when incorporating proteins such as SIgA into the formulation.

SIgA is the predominant immunoglobulin in human colostrum, with concentrations ranging from 1.5 to 83.7 $g \cdot L^{-1}$ [16,17]. Produced locally as a dimer complexed with a secretory component, SIgA plays a critical role in mucosal immunity—neutralizing pathogens, modulating inflammatory responses, and maintaining intestinal homeostasis [18,19].

The immune function of SIgA is mediated by interactions with Fcα receptors, primarily FcαRI (CD89), which are expressed on various myeloid cells, including monocytes, neutrophils, and macrophages [20-22]. Engagement of SIgA with FcαRI triggers processes like phagocytosis, reactive oxygen species production, and cytokine release [23,24].

The secretory component endows SIgA with stability and resistance to bacterial proteases, characteristics that, combined with its effector functions, make it a strong candidate for passive immunotherapy via mucosal routes [24,25]. Therefore, encapsulating SIgA in microemulsions could enhance its stability and bioactivity, while also modulating immune cell function.

Previous studies suggest that colostral macrophages can be stimulated by SIgA via CD89, potentially enhancing defense against enteropathogenic *Escherichia coli* (EPEC), a major cause of pediatric diarrheal disease [23,26]. However, the impact of colostrum-derived SIgA (SIgA-C) on the oxidative metabolism of these phagocytes remains underexplored.

This study aimed to extract SIgA from human colostrum, incorporate it into a microemulsion system, and characterize its physicochemical properties. Furthermore, we investigated the immunomodulatory effects of this system on the oxidative activity of colostral phagocytes challenged with EPEC.

2. Materials and Methods

2.1. Subjects and sample size.

A total of 37 healthy postpartum women receiving care through Brazil's Unified Health System (SUS) were recruited to collect colostrum samples. Eligible participants were between 18 and 35 years of age, had delivered full-term newborns (37–41 weeks of gestation) without malformations, tested negative for syphilis, hepatitis B, hepatitis C, and HIV, were not on continuous medication, and had no chronic conditions such as obesity, hypertension, or diabetes.

Sample size was calculated based on a 10% expected loss and correction for type I (α = 5%) and type II (β = 20%) errors. Participants were invited to donate approximately 8 mL of colostrum collected manually using an appropriate technique in the morning between two feedings, within 48–72 hours postpartum. The sampling and experimental workflow are shown in Figure 1.

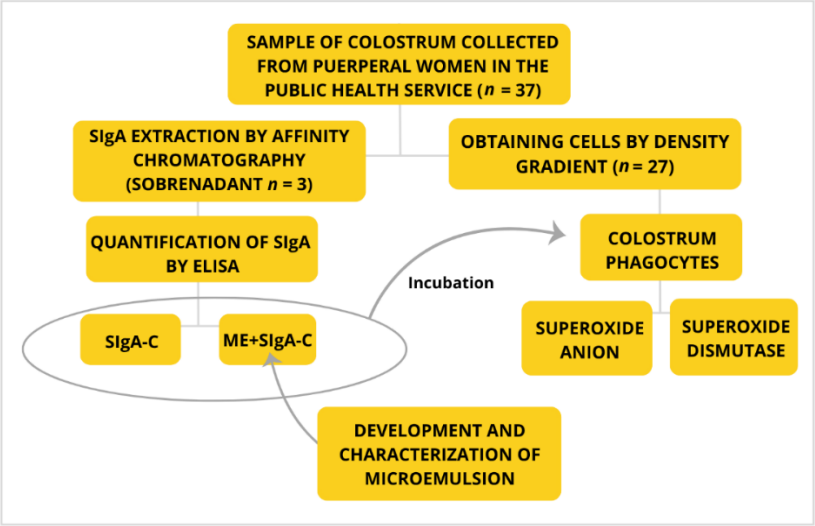

Figure 1. Representative scheme of sample collection and experimental design.

2.2. Preparation of the human colostrum supernatant pool.

Ten colostrum samples were used to prepare the supernatant. Samples were centrifuged at 160 × g for 10 minutes at 4°C. The supernatants were pooled and centrifuged again at 300 × g for 10 minutes to obtain the colostrum supernatant pool. All samples were pre-screened for contamination before SIgA-C extraction.

2.3. SIgA-C extraction and quantification.

SIgA-C was purified from the pooled colostrum via affinity chromatography using cyanogen bromide-activated Sepharose-4B (CNBr-Sepharose-4B; Sigma, St. Louis, USA) conjugated to anti-human α-chain antibodies (from sheep), according to [27]. SIgA-C concentration was determined by Enzyme-Linked Immunosorbent Assay (ELISA). Purity was confirmed by immunoelectrophoresis with goat anti-human γ- and μ-chain antisera, demonstrating the absence of IgG and IgM. The final concentration of SIgA-C was 32 $mg \cdot mL^{-1}$ and was diluted to 100 $ng \cdot mL^{-1}$ for use. Aliquots were stored at −80°C until further experimentation [16].

2.4. Composition of colostrum-derived SIgA-loaded microemulsion (ME+SIgA-C).

The ME+SIgA-C was formulated with an aqueous phase (distilled water), an oil phase composed of capric/caprylic triglycerides (CCT), and a surfactant system consisting of Span 20, Tween 20, and 1-butanol. The final formulation comprised 15% oil phase, 15% aqueous phase, and 70% surfactant mixture [7].

For preparation, 6.096 g of CCT, 9.624 g of Span 20, and 16.200 g of Tween 20 were combined. Subsequently, 5.4 mL of SIgA-C solution (100 ng·mL^{-1}), corresponding to 15% of the aqueous phase, was incorporated in two steps to ensure homogeneous dispersion. Finally, 2.076 g of 1-butanol was added, and the system was homogenized by vigorous vortex mixing after each addition until a uniform microemulsion was obtained.

2.5. Preparation of ME+SIgA-C samples for ELISA-based.

For protein integrity assessment, samples were prepared under standardized conditions and categorized into three experimental groups: (i) free SIgA-C in neutral buffer, serving as a positive control for protein integrity; (ii) microemulsion base (ME), used as a matrix interference control; and (iii) ME+SIgA-C, representing the experimental formulation.

Before analysis, all samples were diluted 1× in 1× phosphate-buffered saline (PBS, pH 7.4) to ensure pH within the optimal assay range (7.2–7.4). To account for potential interference from microemulsion components, serial dilutions (1:50, 1:100, 1:200, and 1:400) were prepared using either the kit-provided sample diluent or PBS supplemented with 1% bovine serum albumin. The same dilution scheme was consistently applied to all experimental groups.

Following dilution, samples were centrifuged at 2000–3000 rpm for 10–15 minutes to promote clarification. The supernatant was carefully collected, avoiding opalescent regions and foam, to minimize optical interference during absorbance reading.

The ELISA assay (Human IgA (Immunoglobulin A) ELISA Kit, Cat. No. E-EL-H6071, Elabscience®, Houston, TX, USA) was performed according to the manufacturer's instructions. SIgA concentrations were determined using the linear portion of the standard curve (12.5–100 ng·mL^{-1}) and linear regression to interpolate sample values within this range. The enzymatic reaction was quantified by measuring absorbance at 450 nm using a microplate spectrophotometer (Thermo Plate TP-Reader, Thermo Fisher Scientific, Waltham, MA, USA). Sample concentrations were calculated based on the immunoglobulin A standard curve and expressed as nanograms per milliliter (ng·mL^{-1}).

2.6. Dynamic light scattering.

Colloidal suspensions of the formulation were prepared for dynamic light scattering analysis. It was then possible to investigate the hydrodynamic diameter of the dispersed solid. The samples were prepared from a 10:1,000 dilution of the formulation in a quartz cuvette using deionized water as the reference. Dynamic light scattering analyses were performed using a Zetasizer Nano Z90® (Malvern Instruments®, Malvern, UK) with excitation at 632.8 nm.

2.7. Physicochemical characterization of ME+SIgA-C.

Initial characterization was conducted 24 hours post-preparation and repeated after the stability study. All tests were performed in triplicate (n = 3).

pH was measured with a calibrated pH meter (PHTEK®; certificate no. 001058/2024) using an electrode inserted directly into the sample. Electrical conductivity was measured with

a conductivity meter (LIDA® DDS-307 W; certificate no. 001057/2024) to determine emulsion type and assess phase inversion potential. Macroscopic appearance was documented photographically [7,28].

2.8. Dilution test for identifying microemulsion (O/W vs W/O).

The type of microemulsion (oil-in-water, O/W, or water-in-oil, W/O) was qualitatively assessed using a dilution test based on the formulation's miscibility in the aqueous and oil phases. O/W systems are characterized by higher affinity and miscibility with water, whereas W/O systems exhibit preferential miscibility in oil. The following formulations were evaluated: ME and ME + SIgA-C. All experiments were performed in independent triplicate.

For the aqueous dilution test, 100 µL of each formulation was added to 900 µL of distilled water (1:10, v/v) in transparent tubes, followed by gentle homogenization by pipetting or low-speed vortexing. The formation of a homogeneous and stable dispersion, without phase separation, visible aggregates, or heterogeneity, was considered indicative of an O/W microemulsion.

For the oil dilution test, 100 µL of each formulation was added to 900 µL of the oil phase (CCT) at a 1:10 (v/v) dilution ratio. After gentle homogenization, miscibility and dispersion stability were evaluated. Limited miscibility, heterogeneous turbidity, aggregate formation, or phase separation were interpreted as behavior consistent with O/W systems and served as a negative control for oil miscibility.

All samples were visually documented immediately after homogenization (time 0) and after 30 minutes of rest. Image acquisition was performed under standardized lighting, background, camera distance, and sample positioning conditions to ensure reproducibility and comparability of the results.

2.9. Preliminary stability study.

ME+SIgA-C were divided into four storage groups: “A” (room temperature, 25 ± 2°C); “G” (refrigerated, 4 ± 1°C – Midea® MD-RT468 MTA012); “E” (heated, 40 ± 2°C – Biopar® S80SA); “CA” (alternating cycles: 24 hours at 4 °C and 24 hours at 40°C, for 14 days) (Figure 2) [7,8,28].

On day 14, all samples were stabilized at room temperature (24 hours) before final physicochemical and rheological evaluations. All tests were performed in triplicate (n = 3).

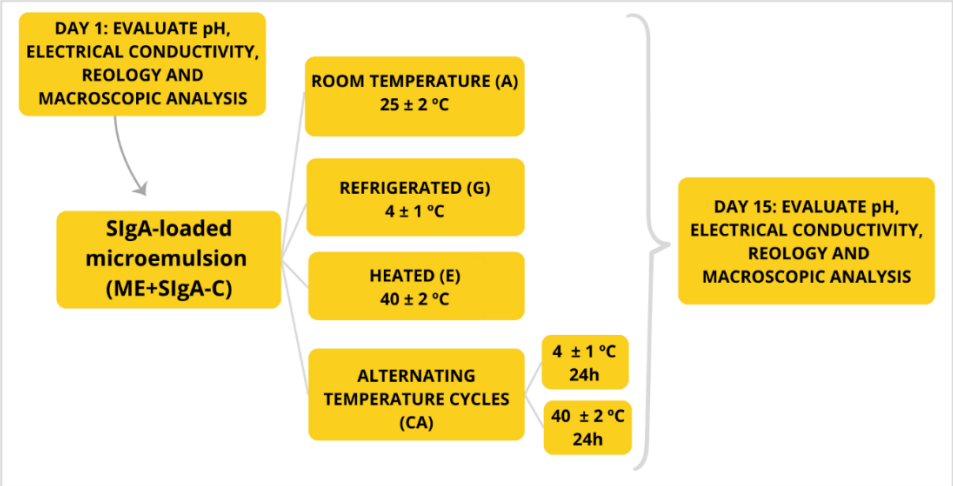

Figure 2. Representative scheme of the preliminary stability study (n=3).

2.10. Rheological characterization.

Rheological measurements were performed using a Rheometer MCR 102 (Anton Paar® GmbH, Ostfildern, Germany) equipped with Rheoplus V3.61 software. The instrument featured TruGap™ (gap set to 0.099 mm), Toolmaster™ CP 50 cell, and T-Ready™ temperature control. Each test used 600 µL of the microemulsion SIgA-containing. Shear stress (τ) ranged from 0 to 5 Pa·s (ascending curve) and from 5 to 0 Pa·s (descending curve). Graphs were generated using Rheoplus software. Tests were conducted in triplicate (n = 3) under isothermal conditions (25°C).

2.11. Isolation of mononuclear cells from human colostrum.

Twenty-seven colostrum samples were centrifuged at 1500 rpm for 10 minutes to separate cells. The supernatant was discarded, and the pellet was resuspended in 5 mL of Medium 199. Mononuclear cells were isolated using a Ficoll-Paque density gradient (1.077; Cytiva, Marlborough, MA, USA) and centrifuged at 1500 rpm for 40 minutes at 4°C.

The mononuclear layer was collected with a Pasteur pipette, washed twice with PBS plus glucose, and resuspended in 1 mL of the same solution. Cell concentration was adjusted to 2×10^6 cells·mL^{-1} using a Neubauer chamber.

2.12. Enteropathogenic Escherichia coli (EPEC) strains and cultures.

EPEC strains (serotype O111:H−AL−, eae$^+$, eaf$^+$, bfp$^+$) were stored at −70°C and maintained on semi-solid agar in the dark. For experiments, subcultures were grown in 8 mL of tryptic soy broth (TSB; Difco) at 37°C for 18 hours. Bacteria were washed twice with PBS and adjusted to 1×10^7 CFU·mL^{-1} (OD = 0.1 at 540 nm).

2.13. Incubation of colostrum phagocytes with ME+SIgA-C.

Colostrum mononuclear cells were incubated for 2 hours at 37°C in 5% CO_2 in the presence of SIgA-C, ME, or ME+SIgA-C, with or without EPEC bacteria.

After incubation, superoxide anion production was assessed, and culture supernatants were collected for analysis of CuZn-superoxide dismutase (SOD). Controls included cells incubated in Medium 199 or PBS under the same conditions.

2.14. Superoxide anion release.

Superoxide anion production was assessed using ferricytochrome C reduction, following the method of [29] adapted by [30]. In this assay, ferricytochrome C is reduced to ferrocytochrome C in the presence of superoxide, detectable colorimetrically.

Phagocytes (2×10^6 cells·mL^{-1}) were incubated with SIgA-C, ME, or ME+SIgA-C (with or without bacteria). Samples were centrifuged at 160 × g for 10 minutes, and the supernatant was collected for SOD activity analysis.

2.15. CuZn-superoxide dismutase (SOD) activity.

SOD activity in supernatants was measured using the nitro blue tetrazolium (NBT) photoreduction assay (SIGMA), as described by [31]. Following cell incubation with SIgA-C, ME, or ME+SIgA-C (with or without bacteria), samples were centrifuged at 160 × g for 10 minutes. Each reaction received: 0.5 mL of hydroalcoholic solution, 0.5 mL of chloroform-

ethanol (1:1), 0.5 mL of an NBT-ethylenediaminetetraacetic acid (EDTA) mixture, and 2.0 mL of carbonate buffer (pH 10.2) containing hydroxylamine. Tubes were incubated in the dark at room temperature for 15 minutes. Absorbance was measured at 560 nm. Enzyme activity was calculated as the difference between the sample and standard absorbance, normalized to the standard value.

2.16. Statistical analysis.

Data were analyzed using Microsoft Excel® and expressed as mean ± standard error of the mean (SEM). The normality of data distribution was assessed using the Shapiro–Wilk test, and homogeneity of variances was evaluated using Levene's test. Statistical analyses were performed using BioEstat v5.0 (Instituto Mamirauá, Belém, Brazil).

For rheological parameters, including flow curves and viscosity measurements of the ME and the ME+SIgA-C, comparisons between the two groups were conducted using Student's t-test, and effect sizes were estimated using Cohen's d. For all other analyses involving three or more groups, such as physicochemical parameters, superoxide production, SOD activity, and the SOD/superoxide ratio, one-way analysis of variance (ANOVA) followed by Tukey's p*ost hoc* test was used, provided the assumptions of normality and homogeneity of variances were met. For these comparisons, effect sizes were estimated using eta-squared (η^2). Statistical significance was defined as $p < 0.05$, and effect sizes were interpreted to complement *p*-values, providing additional information on the magnitude of the observed differences.

3. Results and Discussion

3.1. Extraction of SIgA-C and quantification in the ME+SIgA-C formulation.

The extraction process yielded three eluates containing SIgA-C at varying concentrations, yielding a total protein concentration of 32 mg·mL^{-1}. Before incorporation into the microemulsion system, the SIgA-C concentration was standardized to 100 ng·mL^{-1} to ensure consistency across formulations.

SIgA-C quantification in the ME+SIgA-C formulation was estimated using the standard curve. The ME+SIgA-C formulation exhibited a concentration of 92.03 ng·mL^{-1}. Free SIgA-C showed a value of 101.09 ng·mL^{-1}, while the ME presented a background signal equivalent to 1.07 ng·mL^{-1}.

3.2. Hydrodynamic diameter and zeta potential.

The zeta potential and hydrodynamic diameter of the ME+SIgA-C formulation are presented in Figure 3. The system exhibited a hydrodynamic diameter of approximately 80 nm, remaining within the nanometric range after SIgA incorporation. The DLS profile showed a predominantly unimodal distribution, suggesting that the addition of SIgA-C did not markedly alter the droplet size profile of the microemulsion.

The ζ-potential was approximately −30 mV, indicating moderate to high colloidal stability, likely due to electrostatic repulsion between dispersed droplets, which may reduce the tendency for aggregation and coalescence. These findings suggest that incorporating a high-molecular-weight biomolecule did not substantially alter the system's physicochemical characteristics.

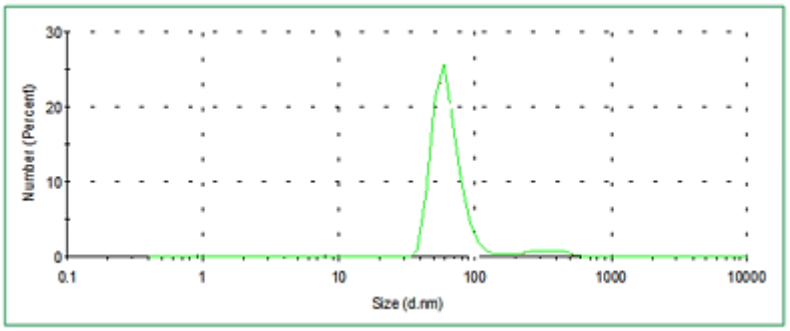

Figure 3. Droplet size distribution of the microemulsion containing colostrum-derived SIgA (ME+SIgA-C) obtained by dynamic light scattering (DLS). The distribution profile shows a predominant unimodal peak centered around 80–100 nm, consistent with a nanometric droplet population. A minor secondary population at larger diameters is observed, likely corresponding to a small fraction of aggregates. The overall profile suggests a relatively homogeneous system.

3.3. Physicochemical characterization.

The physicochemical properties of ME+SIgA-C under preliminary stability conditions are summarized in Table 1. Based on its electrical conductivity, which exceeds that of distilled water (>1.3 $\mu S \cdot cm^{-1}$), the system was classified as an O/W microemulsion. Additionally, the ME+SIgA-C exhibited a pH of 3.93, consistent with the physicochemical stability required for mucosal applications.

Table 1. Physicochemical analysis of the ME+SIgA-C before and after preliminary stability tests (n = 3).

Samples	Appearance	Electrical conductivity ($\mu S \cdot cm^{-1}$)	pH
ME+SIgA-C - Day 1	MEL	53.77 ± 0.04	3.93 ± 0.04
ME+SIgA-C - A15	MEL	44.60 ± 0.73 *	4.07 ± 0.06
ME+SIgA-C - G15	MEL	45.43 ± 0.38 *	4.11 ± 0.06 *
ME+SIgA-C - E15	MEL	45.60 ± 0.00 *	4.01 ± 0.02
ME+SIgA-C - CA15	MEL	44.23 ± 0.18 *	4.21 ± 0.05 *

ME+SIgA-C: Colostrum-derived SIgA-loaded microemulsion; A15: room temperature (25 ± 2°C); G15: refrigerated (4 ± 1°C); E15: heated (40 ± 2°C); CA15: alternating temperature cycles (4°C ↔ 40°C); MEL: liquid microemulsion. Data are expressed as mean ± standard error (n = 3). Statistical comparisons were performed using one-way ANOVA followed by Tukey's *post hoc* test. *Indicates significant differences between post-stability groups (A15, G15, E15 and CA15) and the microemulsion at day 1 (ME+SIgA-C - Day 1). $p < 0.0001$ for electrical conductivity and $p < 0.0067$ for pH.

Figure 4 shows the macroscopic appearance of the ME+SIgA-C on days 1, 15, and 180 after preparation. The first day, the formulation exhibited macroscopic characteristics typical of microemulsions, including translucency, homogeneity, and a liquid appearance. After 15 days of storage, all formulations exhibited macroscopic stability and visual characteristics typical of microemulsions, including translucency, homogeneity, and a liquid appearance, and remained unchanged even after 6 months (Figure 4). Although electrical conductivity decreased across all groups compared to the control formulation (ME+SIgA-C - Day 1), the O/W classification was maintained. No statistically significant changes in pH were detected in samples stored at room temperature (25 ± 2°C) or heated (40 ± 2°C). However, formulations stored under refrigerated (4 ± 1°C) and those subjected to temperature cycles (4 ± 1°C ↔ 40 ± 2°C) showed increased pH values (Table 1).

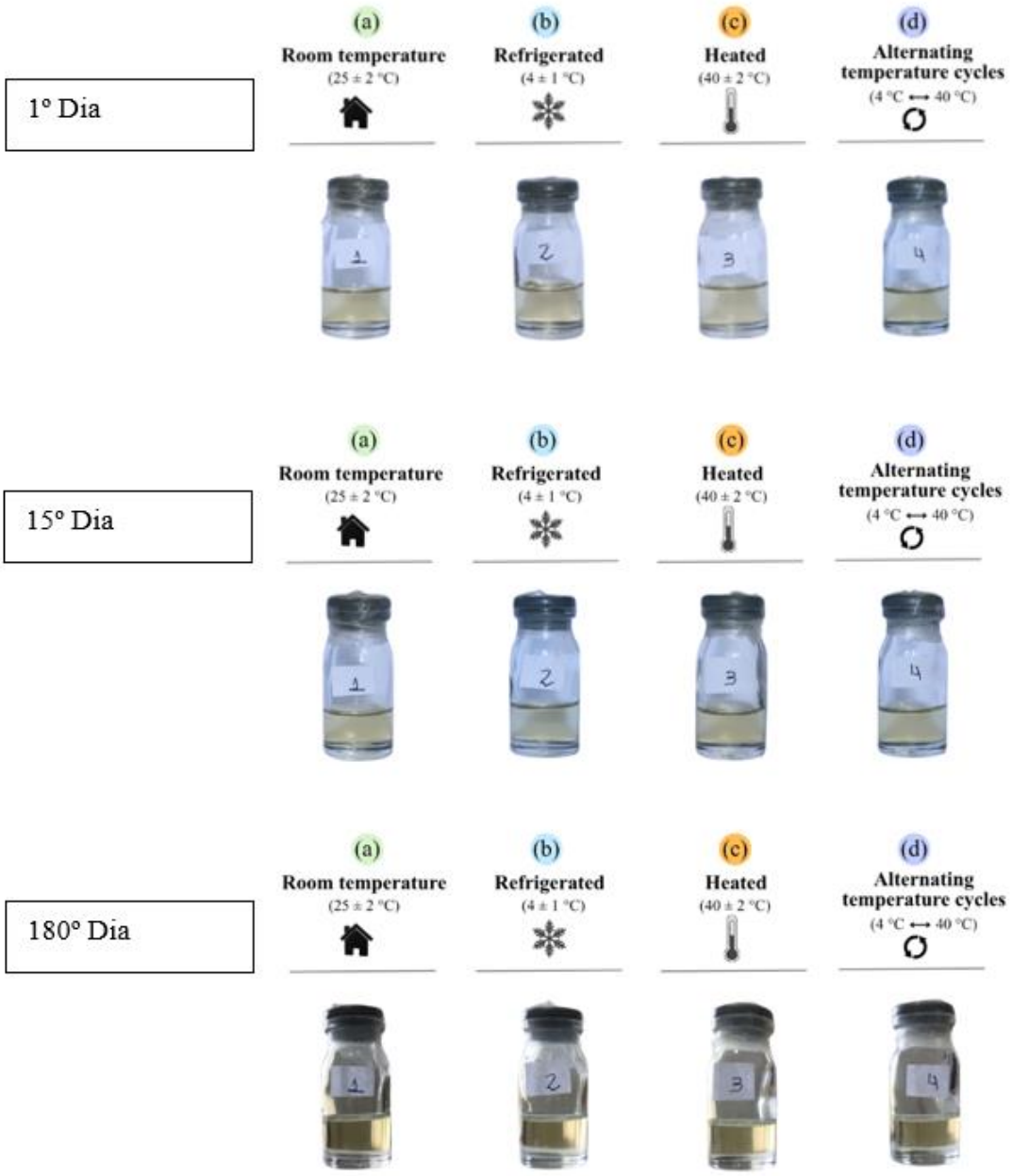

Figure 4. Macroscopic appearance of the colostrum-derived SIgA-loaded microemulsion (ME+SIgA-C) at 1, 15, and 180 days after preparation, evaluated under different storage conditions: **(a)** room temperature (25 ± 2°C); **(b)** refrigerated (4 ± 1°C); **(c)** heated (40 ± 2°C); **(d)** alternating temperature cycles (4°C ↔ 40°C). The images demonstrate preserved visual homogeneity and absence of phase separation or macroscopic instability across all evaluated conditions and time points.

In the dilution test (1:10), both the ME and the ME+SIgA-C exhibited macroscopically homogeneous dispersion in water and CCT, with no visible evidence of phase separation, flocculation, or aggregate formation. The systems maintained a uniform visual appearance immediately after mixing (0 min) and after 30 minutes of rest (Figure 5).

It should be noted that this assessment is based on macroscopic observation and therefore provides qualitative evidence of dispersion behavior, not replacing detailed physicochemical characterization of the internal structure.

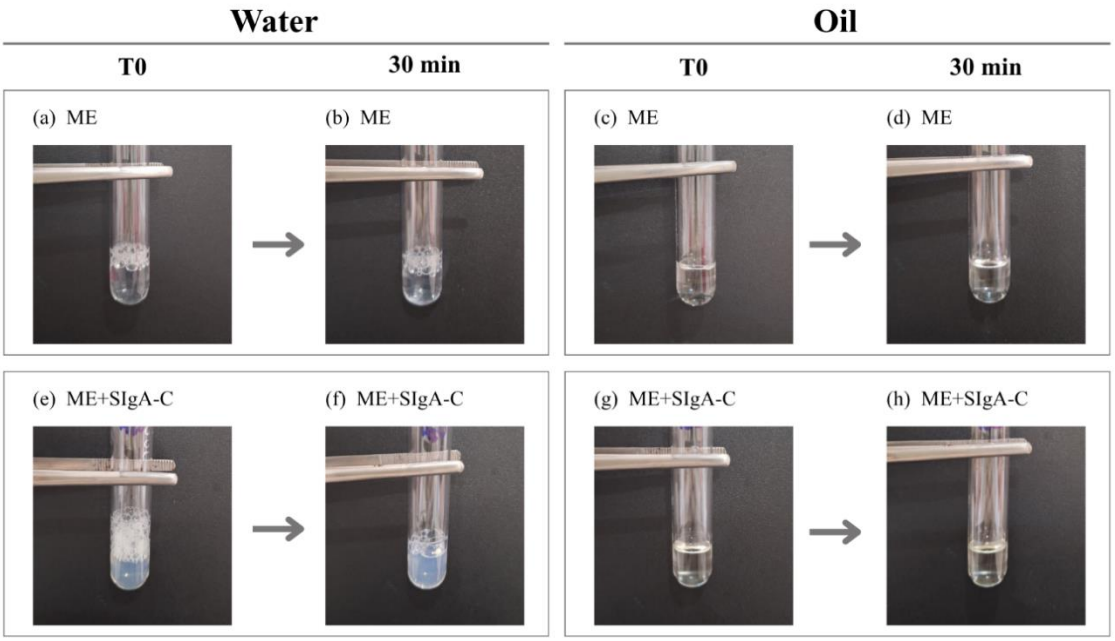

Figura 5. Dilution test (1:10) for evaluation of the macroscopic behavior of the microemulsion base (ME) and colostrum-derived SIgA-loaded microemulsion (ME+SIgA-C) in water and oil caprylic/capric triglycerides (CCT). Images were recorded immediately after mixing (0 min) and after 30 minutes of rest. (**a**, **c**) ME at 0 min: **(a)** diluted in water; **(c)** diluted in CCT; (**b**, **d**) ME after 30 min: **(b)** water; **(d)** CCT. (**e**, **g**) ME+SIgA-C at 0 min: **(e)** diluted in water; **(g)** diluted in CCT; (**f**, **h**) ME+SIgA-C after 30 min: **(f)** water; **(h)** CCT.

3.4. Rheological characterization.

The flow and viscosity curves of the ME+SIgA-C and the ME are presented in Figures 6a and 6b. Both systems exhibited typical Newtonian behavior, characterized by flow curves that originated at zero shear rate and remained linear in both the ascending and descending directions. Viscosity profiles also displayed linear behavior, confirming consistent flow properties. The incorporation of SIgA-C into the ME resulted in a slight increase in shear rate accompanied by a reduction in viscosity; however, key rheological characteristics, such as Newtonian behavior and viscosity linearity, remained unchanged. These findings indicate that the addition of SIgA-C does not compromise the structural integrity or flow properties of the microemulsion system.

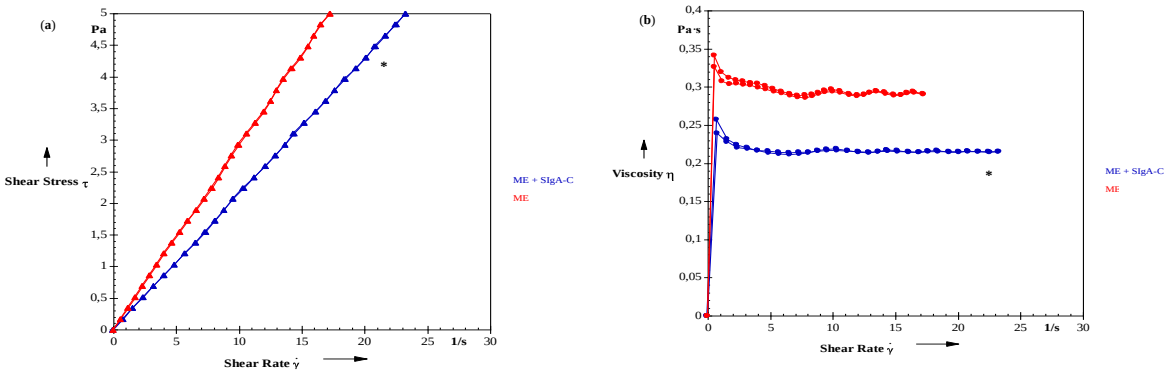

Figure 6. (a) Flow curve; **(b)** viscosity of the colostrum-derived SIgA-loaded microemulsion (ME+SIgA-C) and the microemulsion base (ME) at 25°C. Data are expressed as mean ± standard error (n = 3). Statistical comparisons were performed using the Student's t-test. *p < 0.05 between ME+SIgA-C and ME.

Rheological analysis after the preliminary stability test is presented in Figures 7a and 7b and summarized in Table 2. Flow curves for all groups at the end of the storage period maintained typical Newtonian behavior, with linearity in both ascending and descending directions, originating from zero shear rate (Figure 7a). Viscosity profiles also remained linear

across all conditions. However, all groups exhibited a statistically significant increase in viscosity compared to the ME+SIgA-C formulation on day 1 (Figure 7b), indicating a post-storage elevation.

Among the tested conditions, the formulation stored at room temperature (25 ± 2°C) for 15 days showed the lowest viscosity values and the smallest deviation from baseline (ME+SIgA-C, Day 1). Although these differences reached statistical significance ($p < 0.05$), the magnitude of change was minimal (<4% variation relative to Day 1). Notably, a large effect size (Cohen's d > 10) was observed, suggesting low measurement variability rather than a biologically meaningful alteration. Collectively, these findings indicate that the rheological profile and structural integrity of the microemulsion are preserved after storage.

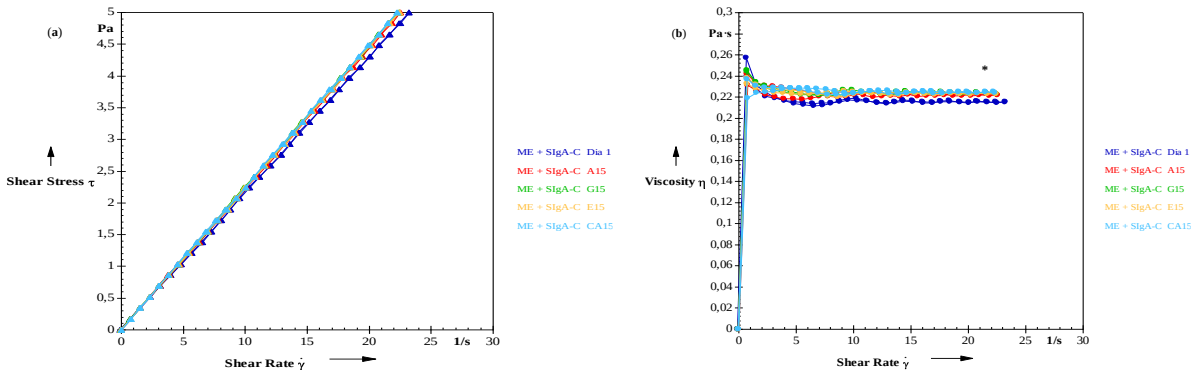

Figure 7. (a) Flow curve; **(b)** viscosity of the colostrum-derived SIgA-loaded microemulsion (ME+SIgA-C) before and after preliminary stability tests (25 °C). Groups: Dia 1 (Day 1); A15: room temperature (25 ± 2 °C); G15: refrigerated (4 ± 1 °C); E15: heated (40 ± 2 °C); CA15: alternating temperature cycles (4 °C ↔ 40 °C). Data are expressed as mean ± standard error ($n = 3$). Statistical comparisons were performed using one-way ANOVA followed by Tukey's *post hoc* test. *Indicates significant differences between post-stability groups (A15, G15, E15 and CA15) and the microemulsion at day 1 (ME+SIgA-C Dia 1). $p = 0.5147$ for shear rate and $p < 0.0001$ for viscosity.

Table 2. Shear rate and viscosity values of the ME+SIgA-C before and after preliminary stability tests ($n = 3$).

Samples	Shear Rate (s^{-1})	Viscosity (Pa·s)
ME+SIgA-C - Day 1	21.41 ± 1.12	0.2151 ± 0.00033
ME+SIgA-C - A15	20.75 ± 1.07	0.2219 ± 0.00066 *
ME+SIgA-C - G15	20.60 ± 1.07	0.2236 ± 0.00058 *#
ME+SIgA-C - E15	20.63 ± 1.06	0.2233 ± 0.00053 *#
ME+SIgA-C - CA15	20.53 ± 1.08	0.2245 ± 0.00050 *#

Notes: ME+SIgA-C: Colostrum-derived SIgA-loaded microemulsion; A15: room temperature (25 ± 2 °C); G15: refrigerated (4 ± 1 °C); E15: heated (40 ± 2 °C); CA15: alternating temperature cycles (4 °C ↔ 40 °C). Data are expressed as mean ± standard error (n = 3). Statistical comparisons were performed using one-way ANOVA followed by Tukey's *post hoc* test. *Indicates significant differences between post-stability groups (A15, G15, E15 and CA15) and the microemulsion at day 1 (ME+SIgA-C – Day 1). #Indicates comparisons among post-stability groups (A15, G15, E15 and CA15). $p = 0.5147$ for shear rate and $p < 0.0001$ for viscosity.

3.5. Effect of ME+SIgA-C on superoxide anion release.

In the oxidative metabolism assays, the ME+SIgA-C from the group stored at room temperature (25 ± 2°C) was used, as it demonstrated the highest stability in the preliminary stability tests. Figure 5 shows the levels of superoxide anion released by colostrum-derived phagocytes following incubation with SIgA-C, ME, and ME+SIgA-C, both in the presence and absence of EPEC bacteria.

Phagocytes treated with ME+SIgA-C exhibited increased superoxide release compared to the spontaneous group, although this release was lower than that observed in cells treated solely with the ME (Figure 8a). Notably, phagocytes incubated only with ME showed the highest levels of superoxide release, surpassing even those exposed to EPEC (Figure 8b).

However, the stimulatory effect of ME was not observed in the presence of the bacteria (Figure 8b), suggesting possible interference or modulation by EPEC. Treatment with SIgA-C alone induced superoxide release levels comparable to the spontaneous group (Figure 8a), and no significant changes in superoxide production were observed in this group in the presence of EPEC (Figure 8b).

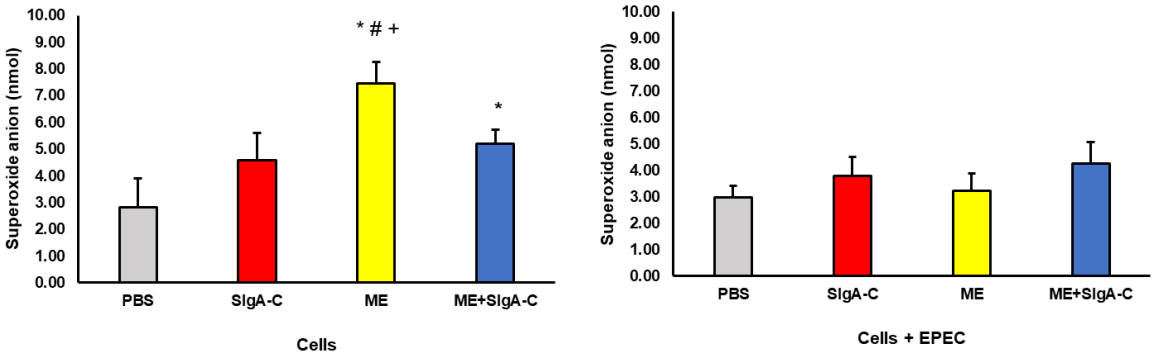

Figure 8. (a) Superoxide anion release by cells treated with colostrum-derived SIgA (SIgA-C), microemulsion base (ME), or colostrum-derived SIgA-loaded microemulsion (ME+SIgA-C); **(b)** Cells were also incubated with enteropathogenic *Escherichia coli* (EPEC) and subsequently treated with SIgA-C, ME, or ME+SIgA-C. Results represent mean ± standard error of 27 colostrum samples. Statistical significance was considered at $p < 0.05$. *Difference between the PBS-treated group and the groups SIgA-C, ME, and ME+SIgA-C. #Difference among the treatments SIgA-C, ME, and ME+SIgA-C. +Difference between cells under the same treatment with or without bacteria.

3.6. Effect of ME+SIgA-C on CuZn-superoxide dismutase (SOD) enzymatic activity.

The concentration of SOD in the culture supernatants of colostrum-derived phagocytes treated with either SIgA-C, ME, or ME+SIgA-C is shown in Figure 9. SOD levels were similar between groups receiving the same treatment, regardless of EPEC exposure. In the presence and absence of bacteria, a reduction in SOD levels was observed in culture supernatants when the ME was present, alone or in combination with the SIgA-C.

Supernatants from cells treated with SIgA-C alone showed SOD concentrations comparable to those of the spontaneous group and the highest among all treatment groups (Figure 9a–9b). In contrast, cells treated with the ME+SIgA-C exhibited the lowest SOD concentrations, suggesting a potential modulatory effect of the formulation on enzyme activity (Figure 9a–9b).

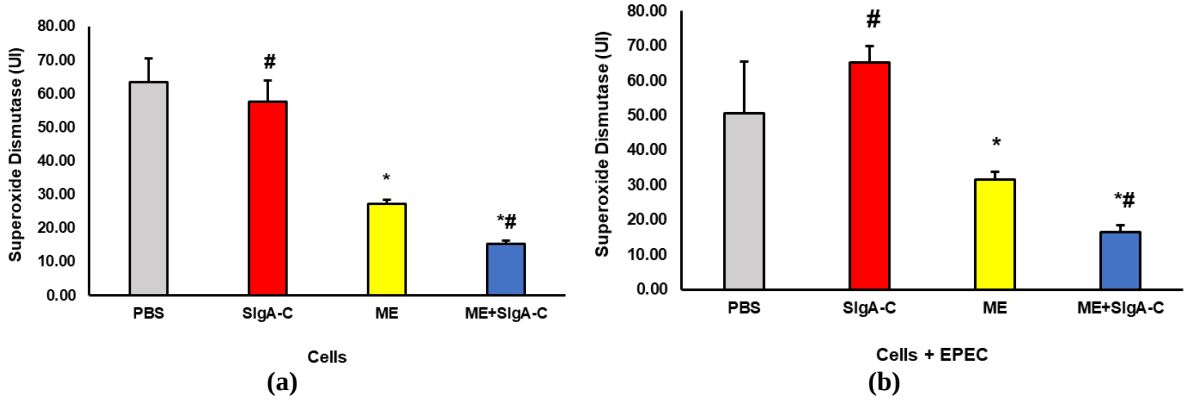

Figure 9. (a) CuZn-superoxide dismutase (SOD) concentration in the culture supernatant of mononuclear phagocytes (MN) from human colostrum. Cells were treated with colostrum-derived SIgA (SIgA-C), microemulsion base (ME), or colostrum-derived SIgA-loaded microemulsion (ME+SIgA-C); **(b)** Cells were also incubated with enteropathogenic *Escherichia coli* (EPEC) and subsequently treated with SIgA-C, ME, or ME+SIgA-C. Results represent mean ± standard error of 27 colostrum samples. Statistical significance was considered at $p < 0.05$. *Difference between the PBS-treated group and the groups SIgA-C, ME, and ME+SIgA-C. #Difference among the treatments SIgA-C, ME, and ME+SIgA-C.

These results suggest that SIgA-C, either alone or incorporated into microemulsions, may influence the levels of SOD in human colostrum phagocytes, potentially regulating oxidative stress in these cells.

3.7. Effect of ME+SIgA-C into microemulsion on the SOD/O_2^- ratio.

The superoxide dismutase/superoxide anion (SOD/O_2^-) ratio in the culture supernatants of human colostrum phagocytes treated with SIgA-C, ME, or ME+SIgA-C, in the presence or absence of EPEC, is shown in Figure 10. All colostrum phagocytes, regardless of treatment, exhibited a reduced SOD/O_2^- ratio. Cells treated with the ME+SIgA-C and ME displayed the lowest SOD/O_2^- ratios among the treatment groups (Figure 10a), whereas cells treated with SIgA-C alone showed the highest ratio.

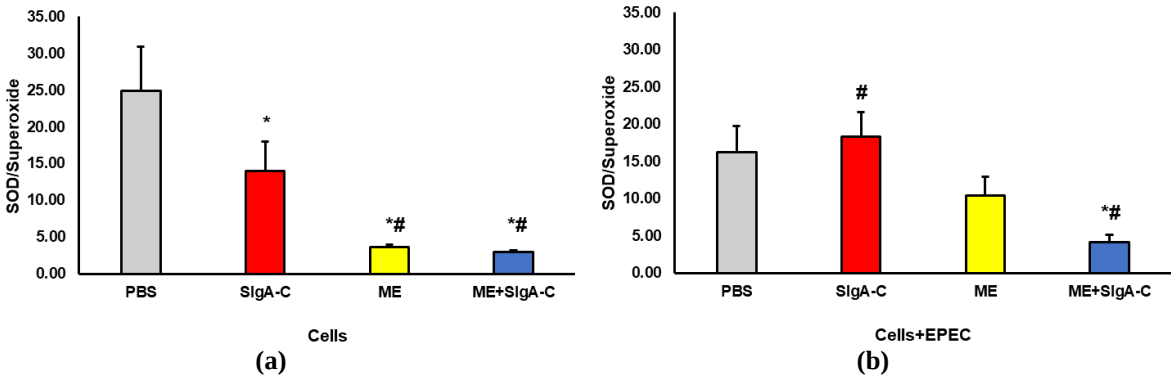

Figure 10. (a) SOD/superoxide ratio in human colostrum mononuclear phagocytes (MN). Cells were treated with colostrum-derived SIgA (SIgA-C), microemulsion base (ME), or colostrum-derived SIgA-loaded microemulsion (ME+SIgA-C); **(b)** Cells were also incubated with enteropathogenic *Escherichia coli* (EPEC) and subsequently treated with SIgA-C, ME, or ME+SIgA-C. Results represent mean ± standard error of 27 colostrum samples. Statistical significance was considered at $p < 0.05$. *Difference between the PBS-treated group and the groups SIgA-C, ME, and ME+SIgA-C. #Difference among the treatments SIgA-C, ME, and ME+SIgA-C.

In the presence of EPEC, colostrum phagocytes treated with ME+SIgA-C exhibited the lowest SOD/O_2^- ratio. In contrast, cells treated with SIgA-C alone showed the highest ratio among all treated groups, with values comparable to those of the control group (Figure 10b).

3.8. Discussion.

In this study, SIgA-C was obtained at a concentration of 32 mg·mL^{-1}, indicating high extraction efficiency. The purified SIgA-C was successfully incorporated into an oil-in-water microemulsion system composed of Span, Tween, and Butanol, resulting in a translucent, homogeneous liquid formulation with an acidic pH and Newtonian flow behavior. The purified SIgA-C was successfully incorporated into an oil-in-water microemulsion system composed of Span/Tween/Butanol, showing a translucent, homogeneous, and liquid formulation with an acidic pH and Newtonian flow behavior. Despite the observed increase in shear rate and a corresponding decrease in viscosity following SIgA-C incorporation, the system maintained its overall rheological profile. This behavior likely reflects interactions between SIgA-C and surfactant molecules, leading to rearrangement of micellar or droplet structures and reducing internal resistance to flow, as previously reported in similar systems [32,33].

Microemulsions generally exhibit Newtonian behavior, and this behavior was preserved after SIgA-C incorporation, in agreement with previous reports showing that the addition of drugs, oils, or plant extracts did not significantly alter rheological properties [7,28,33]. This consistency in flow behavior supports the potential of microemulsions as

delivery systems for bioactive macromolecules, particularly for mucosal and topical administration, where constant viscosity is essential for formulation stability, spreadability, and ease of application. The formulation also maintained detectable levels of SIgA-C. The ME+SIgA-C concentrations were within the expected range, indicating that the incorporation process did not compromise antibody detectability. These findings suggest that the structural and functional integrity of SIgA-C was preserved within the microemulsion system, especially in antigen-antibody recognition. The maintenance of immunoreactivity supports the suitability of the formulation as a carrier for sensitive biomolecules such as immunoglobulins, in agreement with previous studies [7,13,14].

The incorporation of SIgA-C, a predominantly hydrophilic macromolecule, is expected to influence the interfacial organization of the microemulsion system. Due to its amphiphilic nature and structural complexity, SIgA-C is likely to localize at or near the oil–water interface, where it interacts with surfactant molecules and contributes to interfacial stabilization. This behavior may explain the maintenance of nanoscale droplet size despite protein incorporation.

High absolute values of ζ-potential, as observed in this study, are commonly associated with stable colloidal dispersions, as they reduce the likelihood of droplet aggregation through electrostatic repulsion [32,7]. The negative ζ-potential observed may be related to the formulation's physicochemical properties, including pH and the presence of ionizable groups at the droplet surface. Under such conditions, increased negative surface charge contributes to enhanced dispersion stability [32,13].

Stability testing over 15 days demonstrated that the ME+SIgA-C maintained macroscopic homogeneity, translucency, and the typical appearance of liquid microemulsions under all tested conditions. This profile remained unchanged after 180 days of storage, with no visible signs of phase separation or instability.

Electrical conductivity values above 1.3 $\mu S \cdot cm^{-1}$ confirmed the oil-in-water character of the formulations [34, 8, 14], including those containing SIgA-C. Although conductivity decreased slightly in all groups over time, likely due to water loss or rearrangement of internal structures, no phase inversion or visual destabilization occurred, a favorable outcome for formulation stability and potentially contributing to bioavailability.

The pH remained stable at room temperature ($25 \pm 1°C$) and at heated ($40 \pm 1°C$) conditions, but increased in refrigerated ($5 \pm 1°C$) and temperature-cycled samples. This rise in pH may reflect the release of peptide fragments or conformational alterations in SIgA-C, which are known to occur in protein-based systems under certain storage conditions [35,36]. Monitoring pH changes is critical, as they may indicate hydrolysis of triglycerides, oxidation of the oil phase, or degradation of SIgA-C, all of which can compromise immunological function [35,14,33].

The system exhibited an acidic pH, which is particularly relevant considering the gastrointestinal environment targeted for SIgA activity. The gastrointestinal tract presents a highly dynamic pH gradient, ranging from strongly acidic conditions in the stomach (pH 1.5–3.5) to near-neutral or slightly alkaline values in the intestine (pH 6–8). These variations, influenced by factors such as food intake, physiology, and disease states, can promote protein unfolding, conformational changes, and enzymatic degradation, potentially compromising protein bioactivity [37,38].

SIgA is particularly adapted to function at mucosal surfaces, where it plays a key role in immune exclusion and pathogen neutralization. This immunoglobulin contains a secretory component that enhances its resistance to low pH and proteolysis, supporting its stability along

the gastrointestinal tract [39]. However, studies with monoclonal SIgA indicate that extreme acidic conditions (e.g., pH ~3.0) may still affect conformational stability [19].

In the present study, the SIgA-C remained detectable after incorporation into the microemulsion, with concentrations within the expected range, indicating preservation of antibody integrity at the level of antigen–antibody recognition.

Rheological evaluations were performed in triplicate ($n = 3$). No significant differences were observed for shear rate ($p = 0.5147$), whereas viscosity showed a statistically significant variation ($p < 0.0001$). After storage, the absence of hysteresis and the preservation of Newtonian behavior were confirmed. Although statistical significance was detected, the increase in viscosity was minimal, ranging from approximately 3% to 4.4% relative to the initial formulation, without altering the flow profile. These findings indicate that the system's physicochemical stability was maintained over the evaluated period.

Given the limited sample size and the small magnitude of variation, these differences should be interpreted cautiously regarding biological relevance. Notably, the large effect size observed for viscosity reflects the low measurement variability rather than a meaningful structural or functional change. Despite statistical significance, the absolute variation remained minimal, supporting the preservation of the rheological profile and suggesting that these changes are unlikely to impact the functional performance of the microemulsion.

The combination of surfactants employed provided a hydrophilic–lipophilic balance suitable for stabilizing CCT, favoring the formation of small droplet sizes and enhanced thermodynamic stability [40,8,28]. However, the direct relationship between these physicochemical properties and potential biological effects, such as prolonged mucosal retention, controlled release, or macrophage uptake, requires confirmation through dedicated biological assays [7,41,42].

Among the tested storage conditions, the ME+SIgA-C maintained at room temperature exhibited the least variation in viscosity and shear rate, suggesting this condition best preserves the physicochemical integrity of the system. This finding may have practical implications for mucosal delivery platforms, especially in settings where refrigeration is not feasible. Viscosity is a critical factor in mucosal adhesion, retention, and local bioavailability, all of which contribute to the therapeutic performance of immunoglobulin-based formulations [36].

SIgA is a multimeric, glycosylated antibody composed of two IgA monomers linked by a joining (J) chain and associated with a secretory component. The high degree of glycosylation plays a fundamental role in both physical properties and biological activity, including antigen binding and immune regulation [19]. The maintenance of physicochemical and rheological properties following incorporation into the microemulsion system suggests preservation of functional activity, with no evidence of physicochemical destabilization.

After selecting the room-temperature ME+SIgA-C variant based on its superior stability profile, the immunological functionality of SIgA-C was evaluated using colostral phagocytes. The ME+SIgA-C modulated oxidative metabolism, as evidenced by changes in superoxide anion production and SOD activity. These findings suggest that the immunological activity of SIgA-C was preserved after incorporation and storage. Interestingly, the ME stimulated the highest levels of superoxide anion release, even exceeding those observed in EPEC-stimulated cells. This unexpected response suggests that the formulation vehicle may activate oxidative pathways independently, possibly via pattern recognition receptors or mild pro-oxidative mechanisms. This finding highlights the importance of evaluating vehicle effects separately, especially in immunologically active systems.

The ME induced measurable oxidative activity in the cellular assays, indicating that it is not an inert vehicle. This effect is likely due to interactions between the amphiphilic components of the formulation and the cellular membrane. Surfactants and co-surfactants present in microemulsion systems are known to alter membrane fluidity and permeability, thereby transiently activating signaling pathways related to oxidative metabolism in immune cells [4]. Consistent with this, the observed increase in superoxide production and the reduction in the SOD/O_2^- ratio indicate a shift toward a pro-oxidative phenotype, potentially mediated by nicotinamide adenine dinucleotide phosphate (NADPH) oxidase–dependent mechanisms [4,43,44].

In contrast, SIgA-C alone maintained a near-basal redox profile, and its incorporation into the microemulsion did not exacerbate oxidative activity, suggesting that the antibody contributes to regulating the system. In the presence of EPEC, the persistence of a reduced SOD/O_2^- ratio in the ME+SIgA-C group indicates maintenance of an oxidatively activated phenotype, which may be functionally relevant for antimicrobial activity.

Taken together, these findings suggest that the ME may transiently enhance the oxidative effector functions of phagocytes, rather than acting solely as a passive delivery platform. When associated with SIgA-C, this effect appears more regulated. However, further studies are required to determine whether this response is functionally protective.

The observed changes in superoxide production and SOD activity suggest that the formulation may influence cellular redox balance. However, these findings alone do not establish a specific immunomodulatory mechanism.

In contrast, the ME+SIgA-C formulation appears to modulate the oxidative burst, consistent with SIgA's immunomodulatory properties, which regulate phagocytosis, cytokine production, and oxidative responses [25,45]. These results further support the potential of microemulsions as delivery platforms capable of preserving the functional properties of mucosal immunoglobulins.

Taken together, the findings support the feasibility of using microemulsion systems to deliver SIgA-C, suggesting preservation of physicochemical stability and immunological functionality. Future studies should focus on long-term stability, *in vivo* mucosal retention, and protective efficacy against specific pathogens to fully establish the therapeutic potential of this delivery strategy.

4. Conclusions

This study demonstrates that SIgA-C can be efficiently isolated and incorporated into an O/W microemulsion system, exhibiting Newtonian flow behavior and consistent viscosity. The ME+SIgA-C preserved immunological activity, as indicated by the modulation of superoxide anion production and SOD activity in colostral phagocytes. These findings suggest that microemulsified SIgA-C may serve as a promising platform for delivering mucosal immune components. However, further studies, including *in vivo* validation, structural characterization, and long-term stability analyses, are required to confirm its potential applicability in immunotherapeutic strategies targeting bacterial infections and other mucosal diseases.

Author Contributions

Conceptualization, V.F.L., E.L.F. and A.C.H.-F.; methodology, V.F.L., K.M.R.S., N.C.S.A. and A.C.M.C.; validation, V.F.L., K.M.R.S., N.C.S.A. and A.C.M.C.; formal analysis, V.F.L., E.L.F., A.C.M.C. and A.C.H.-F.; data curation, V.F.L., K.M.R.S., N.C.S.A., E.L.F., A.C.M.C. and A.C.H.-F.; writing—original draft preparation, V.F.L., E.L.F. and A.C.H.-F.; writing—review and editing, E.L.F. and A.C.H.-F.; supervision, E.L.F. and A.C.H.-F.; funding acquisition, E.L.F. and A.C.H.-F. All authors have read and agreed to the published version of the manuscript.

Institutional Review Board Statement

The study adhered to the Declaration of Helsinki and was approved by the Araguaia Research Ethics Committee at the Federal University of Mato Grosso, Brazil. An informed consent statement was provided. The study received approval from the Research Ethics Committee (CAAE: 66496523.5.0000.5587). The subjects provided written informed consent before participating in the experimental protocol.

Informed Consent Statement

Informed consent was obtained from all subjects involved in the study. Colostrum samples were collected from healthy voluntary donors after written informed consent was obtained, in accordance with the principles of the Declaration of Helsinki.

Data Availability Statement

The authors will make the data supporting this study's interpretations available if requested.

Funding

The Fundação de Amparo financed this study, a Pesquisa do Estado de Mato Grosso (FAPEMAT) process number Nº000253/2023; Coordenação de Aperfeiçoamento de Pessoal de Nível Superior - Brazil (CAPES), and Conselho Nacional de Desenvolvimento Científico e Tecnológico (CNPq - No 312511/2023-0; No 312841/2023-0), Brazil, and for providing grants to the study.

Acknowledgments

All stages of the study, including study design, data collection, laboratory analyses, statistical analyses, interpretation of results, manuscript preparation, and revision, were performed exclusively by the authors. No external administrative, technical, editorial, or institutional assistance was received.

Conflicts of Interest

The authors declare that the research was conducted without any commercial or financial relationships that could pose a potential conflict of interest.

Abbreviations

The following abbreviations are used in this manuscript:

Abbreviation	Definition
CCT	Caprylic/Capric Triglycerides
EDTA	Ethylenediaminetetraacetic Acid
ELISA	Enzyme-Linked Immunosorbent Assay
EPEC	Enteropathogenic *Escherichia coli*
ME	Microemulsion Base
ME+SIgA-C	SIgA-Loaded Microemulsion
ME+SIgA-C A15	SIgA-Loaded Microemulsion Stored At Room Temperature (25 ± 2°C)
ME+SIgA-C CA15	SIgA-Loaded Microemulsion Stored In Alternating Temperature Cycles (4°C ↔ 40°C)
ME+SIgA-C E15	SIgA-Loaded Microemulsion Stored At Heated (40 ± 2°C)
ME+SIgA-C G15	Siga-Loaded Microemulsion Stored At Refrigerated (4 ± 1°C)
MEL	Liquid Microemulsion
NADPH	Nicotinamide adenine dinucleotide phosphate
NBT	Nitroblue Tetrazolium
O/W	Oil-in-Water
PBS	Phosphate-Buffered Saline
SIgA	Secretory Immunoglobulin A
SIgA-C	Colostrum-Derived SIgA
SOD	Cuzn - Superoxide Dismutase
SOD/O_2^-	Superoxide Dismutase/Superoxide Anion
SUS	Unified Health System
SPAN	Sorbitan Oleate
TWEEN	Polysorbate
W/O	Water-in-Oil

References

1. Soares, T.A.; Torres, A.H.F.; Dalcin, L.D.L.; Gonçalves, L.C.O.; de Magalhães Neto, A.M.; Honorio-Franca, A.C.; Ribeiro, E.B.; França, E.L. Modified Caffeine Release System and Its Immunomodulatory Effects on Breast Tumor Cells and Blood Phagocytes. *Adv. Biol. Chem.* **2023**, *13*, 25-41, https://doi.org/10.4236/abc.2023.131003.
2. Ashique, S.; Sandhu, N.K.; Chawla, V.; Chawla, P.A. Targeted Drug Delivery: Trends and Perspectives. *Curr. Drug Deliv.* **2021**, *18*, 1435–1455, https://doi.org/10.2174/1567201818666210609161301.
3. Zhang, Y.; Chan, H.F.; Leong, K.W. Advanced materials and processing for drug delivery: The past and the future. *Adv. Drug Deliv. Rev.* **2013**, *65*, 104-120, https://doi.org/10.1016/j.addr.2012.10.003.
4. Egito, E.S.T.; Amaral-Machado, L.; Alencar, E.N.; Oliveira, A.G. Microemulsion systems: from the design and architecture to the building of a new delivery system for multiple-route drug delivery. *Drug Deliv. Transl. Res.* **2021**, *11*, 2108-2133, https://doi.org/10.1007/s13346-020-00872-8.
5. Souto, E.B.; Cano, A.; Martins-Gomes, C.; Coutinho, T.E.; Zielińska, A.; Silva, A.M. Microemulsions and Nanoemulsions in Skin Drug Delivery. *Bioengineering* **2022**, *9*, 158, https://doi.org/10.3390/bioengineering9040158.
6. Nikolaev, B.; Yakovleva, L.; Fedorov, V.; Li, H.; Gao, H.; Shevtsov, M. Nano- and Microemulsions in Biomedicine: From Theory to Practice. *Pharmaceutics* **2023**, *15*, 1989, https://doi.org/10.3390/pharmaceutics15071989.
7. Ribeiro, E.B.; Lanes, P.K.D.; Chaud, N.G.A.; Pessoa, R.S.; Honorio-Franca, A.C.; França, E.L. Microemulsions with levamisole delivery systems as novel immunomodulating agents with potential for amebiasis therapies. *Sci. Adv. Mater.* **2015**, *7*, 15-27, https://doi.org/10.1166/sam.2015.2003.
8. Gustmanna, P.C.; de Melo Cotrimb, A.C.; Piresc, E.M.; Andrighettid, C.R.; Valladãod, D.M.S.; Ribeirod, E.B. Development of Brazil nut oil microemulsion as vehicle for Levamisole. *J. Appl. Pharm. Sci.* **2017**, *7*, 092-098, https://doi.org/10.7324/JAPS.2017.70813.
9. Boonme, P.; Krauel, K.; Graf, A.; Rades, T.; Junyaprasert, V.B. Characterization of microemulsion structures in the pseudoternary phase diagram of isopropyl palmitate/water/Brij 97:1-butanol. *AAPS PharmSciTech* **2006**, *7*, 45, https://doi.org/10.1208/pt070245.
10. Leanpolchareanchai, J.; Teeranachaideekul, V. Topical Microemulsions: Skin Irritation Potential and Anti-Inflammatory Effects of Herbal Substances. *Pharmaceuticals* **2023**, *16*, 999, https://doi.org/10.3390/ph16070999.

11. Foo, K.S.; Bavoh, C.B.; Lal, B.; Mohd Shariff, A. Rheology Impact of Various Hydrophilic-Hydrophobic Balance (HLB) Index Non-Ionic Surfactants on Cyclopentane Hydrates. *Molecules* **2020**, *25*, 3725, https://doi.org/10.3390/molecules25163725.
12. Silva, J.D.F.d.; Silva, Y.P.d.; Piatnicki, C.M.S.; Boeckel, W.J.; Mendonça, C.R.B. Microemulsions: components, characteristics, potentialities in food chemistry and other applications. *Quím. Nova* **2015**, *38*, 1196–1206, https://doi.org/10.5935/0100-4042.20150135.
13. Ribeiro, E.B.; de Marchi, P.G.F.; Honorio-Franca, A.C.; França, E.L.; Soler, M.A.G. Interferon-gamma carrying nanoemulsion with immunomodulatory and anti-tumor activities. *J. Biomed. Mater. Res. A* **2020**, *108*, 234-245, https://doi.org/10.1002/jbm.a.36808.
14. Torres, M.D.P.R.; Esprendor, R.V.D.F.; Bonaldo, S.M.; Ribeiro, E.B.; Valladão, D.M.D.S. Development, characterization and stability of microemulsionated formulations of bacaba, *Oenocarpus bacaba* oil. *Acta Amaz.* **2019**, *49*, 246-255, https://doi.org/10.1590/1809-4392201802702.
15. Shi, M.; McHugh, K.J. Strategies for overcoming protein and peptide instability in biodegradable drug delivery systems. *Adv. Drug Deliv. Rev.* **2023**, *199*, 114904, https://doi.org/10.1016/j.addr.2023.114904.
16. Honorio-Franca, A.C.; Fernandes, R.T.S.; Tozetti, I.A.; Fujimori, M.; de Pinho, C.L.C.; Fagundes-Triches, D.L.G. Mechanism anti-tumor of IgA-based delivery system on the human colostral mononuclear cells via Fcα receptor. *Biointerface Res. Appl. Chem* **2021**, *11*, 14906-14917, https://doi.org/10.33263/BRIAC116.1490614917.
17. Donald, K.; Petersen, C.; Turvey, S.E.; Finlay, B.B.; Azad, M.B. Secretory IgA: Linking microbes, maternal health, and infant health through human milk. *Cell Host Microbe* **2022**, *30*, 650-659, https://doi.org/10.1016/j.chom.2022.02.005.
18. Corthésy, B. Role of secretory IgA in infection and maintenance of homeostasis. *Autoimmun. Rev.* **2013**, *12*, 661–665, https://doi.org/10.1016/j.autrev.2012.10.012.
19. Hu, Y.; Kumru, O.S.; Xiong, J.; Antunez, L.R.; Hickey, J.; Wang, Y.; Cavacini, L.; Klempner, M.; Joshi, S.B.; Volkin, D.B. Preformulation Characterization and Stability Assessments of Secretory IgA Monoclonal Antibodies as Potential Candidates for Passive Immunization by Oral Administration. *J. Pharm. Sci.* **2020**, *109*, 407-421, https://doi.org/10.1016/j.xphs.2019.07.018.
20. Monteiro, R.C.; Kubagawa, H.; Cooper, M.D. Cellular distribution, regulation, and biochemical nature of an Fc alpha receptor in humans. *J. Exp. Med.* **1990**, *171*, 597–613, https://doi.org/10.1084/jem.171.3.597.
21. Aleyd, E.; Heineke, M.H.; van Egmond, M. The era of the immunoglobulin A Fc receptor FcαRI; its function and potential as target in disease. *Immunol. Rev.* **2015**, *268*, 123-138, https://doi.org/10.1111/imr.12337.
22. Breedveld, A.; van Egmond, M. IgA and FcαRI: Pathological Roles and Therapeutic Opportunities. *Front. Immunol.* **2019**, *10*, 553, https://doi.org/10.3389/fimmu.2019.00553.
23. FrançA, E.L.; Morceli, G.; Fagundes, D.L.G.; Rudge, M.V.C.; Calderon, I.D.M.P.; Honorio-Franca, A.C. Secretory IgA–Fcα receptor interaction modulating phagocytosis and microbicidal activity by phagocytes in human colostrum of diabetics. *APMIS* **2011**, *119*, 710-719, https://doi.org/10.1111/j.1600-0463.2011.02789.x.
24. Ding, L.; Chen, X.; Cheng, H.; Zhang, T.; Li, Z. Advances in IgA glycosylation and its correlation with diseases. *Front. Chem.* **2022**, *10*, 974854, https://doi.org/10.3389/fchem.2022.974854.
25. de Sousa-Pereira, P.; Woof, J.M. IgA: Structure, Function, and Developability. *Antibodies* **2019**, *8*, 57, https://doi.org/10.3390/antib8040057.
26. Mare, A.D.; Ciurea, C.N.; Man, A.; Tudor, B.; Moldovan, V.; Decean, L.; Toma, F. Enteropathogenic *Escherichia coli*—A Summary of the Literature. *Gastroenterol. Insights* **2021**, *12*, 28-40, https://doi.org/10.3390/gastroent12010004.
27. March, S.C.; Parikh, I.; Cuatrecasas, P. A simplified method for cyanogen bromide activation of agarose for affinity chromatography. *Anal. Biochem.* **1974**, *60*, 149-152, https://doi.org/10.1016/0003-2697(74)90139-0.
28. Pessoa, R.S.; França, E.L.; Ribeiro, E.B.; Lanes, P.K.D.; Chaud, N.G.A.; Moraes, L.C.A.; Honorio-Franca, A.C. Microemulsion of babassu oil as a natural product to improve human immune system function. *Drug Des. Devel. Ther.* **2014**, *9*, 21-31, https://doi.org/10.2147/DDDT.S73756.
29. Pick, E.; Mizel, D. Rapid microassays for the measurement of superoxide and hydrogen peroxide production by macrophages in culture using an automatic enzyme immunoassay reader. *J. Immunol. Methods* **1981**, *46*, 211–226, https://doi.org/10.1016/0022-1759(81)90138-1.

30. Honorio-Franca, A.C.; Carvalho, M.P.S.M.; Isaac, L.; Trabulsi, L.R.; Carneiro-Sampaio, M.M.S. Colostral Mononuclear Phagocytes are Able to Kill Enteropathogenic *Escherichia coli* Opsonized with Colostral IgA. *Scand. J. Immunol.* **1997**, *46*, 59-66, https://doi.org/10.1046/j.1365-3083.1997.d01-86.x.
31. França, E.L.; Nicomedes, T.d.R.; Calderon, I.d.M.P.; França, A.C.H. Time-dependent alterations of soluble and cellular components in human milk. *Biol. Rhythm Res.* **2010**, *41*, 333-347, https://doi.org/10.1080/09291010903407441.
32. Lawrence, M.J.; Rees, G.D. Microemulsion-based media as novel drug delivery systems. *Adv. Drug Deliv. Rev.* **2012**, *64*, 175–193, https://doi.org/10.1016/j.addr.2012.09.018.
33. Debiasi, B.W.; Dourado, S.H.A.; Andrighetti, C.R.; Ribeiro, E.B.; Battirola, L.D.; Valladão, D.M.d.S. Incorporation of *Cordia glabrata* (Mart.) A. DC. extract in microemulsions and their potential antioxidant, photoprotective and virucidal activities. *Braz. J. Biol.* **2022**, *84*, e259451, https://doi.org/10.1590/1519-6984.259451.
34. Bumajdad, A.; Eastoe, J. Conductivity of water-in-oil microemulsions stabilized by mixed surfactants. *J. Colloid Interface Sci.* **2004**, *274*, 268–276, https://doi.org/10.1016/j.jcis.2003.12.050.
35. Tadros, T.; Izquierdo, P.; Esquena, J.; Solans, C. Formation and stability of nano-emulsions. *Adv. Colloid Interface Sci.* **2004**, *108-109*, 303-318, https://doi.org/10.1016/j.cis.2003.10.023.
36. Li, Y.; Jin, L.; Chen, T. The Effects of Secretory IgA in the Mucosal Immune System. *Biomed. Res. Int.* **2020**, *2020*, 2032057, https://doi.org/10.1155/2020/2032057.
37. Zhu, Q.; Chen, Z.; Paul, P.K.; Lu, Y.; Wu, W.; Qi, J. Oral delivery of proteins and peptides: Challenges, status quo and future perspectives. *Acta Pharm. Sin. B* **2021**, *11*, 2416-2448, https://doi.org/10.1016/j.apsb.2021.04.001.
38. Koziolek, M.; Grimm, M.; Becker, D.; Iordanov, V.; Zou, H.; Shimizu, J.; Wanke, C.; Garbacz, G.; Weitschies, W. Investigation of pH and Temperature Profiles in the GI Tract of Fasted Human Subjects Using the Intellicap® System. *J. Pharm. Sci.* **2015**, *104*, 2855-2863, https://doi.org/10.1002/jps.24274.
39. Göritzer, K.; Strasser, R.; Ma, J.K.-C. Stability Engineering of Recombinant Secretory IgA. *Int. J. Mol. Sci.* **2024**, *25*, 6856, https://doi.org/10.3390/ijms25136856.
40. Aboofazeli, R.; Barlow, D.J.; Lawrence, M.J. Particle size analysis of concentrated phospholipid microemulsions: I. Total intensity light scattering. *AAPS PharmSci* **2000**, *2*, 13, https://doi.org/10.1208/ps020213.
41. França, E.L.; Ribeiro, E.B.; Scherer, E.F.; Cantarini, D.G.; Pessôa, R.S.; França, F.L.; Honorio-Franca, A.C. Effects of *Momordica charantia* L. on the Blood Rheological Properties in Diabetic Patients. *Biomed Res. Int.* **2014**, *2014*, 840379, https://doi.org/10.1155/2014/840379.
42. Heurtault, B.; Saulnier, P.; Pech, B.; Proust, J.-E.; Benoit, J.-P. Physico-chemical stability of colloidal lipid particles. *Biomaterials* **2003**, *24*, 4283-4300, https://doi.org/10.1016/s0142-9612(03)00331-4.
43. Frenis, K.; Kuntic, M.; Hahad, O.; Bayo Jimenez, M.T.; Oelze, M.; Daub, S.; Steven, S.; Münzel, T.; Daiber, A. Redox Switches in Noise-Induced Cardiovascular and Neuronal Dysregulation. *Front. Mol. Biosci.* **2021**, *8*, 784910, https://doi.org/10.3389/fmolb.2021.784910.
44. Bianchini, B.H.S.; Martelossi-Cebinelli, G.; Carneiro, J.A.; Rasquel-Oliveira, F.S.; Casagrande, R.; Verri, W.A. Superoxide Anion Generation, Its Pathological Cellular and Molecular Roles and Pharmacological Targeting in Inflammatory Pain: Lessons from the Potassium Superoxide Model. *Future Pharmacol.* **2025**, *5*, 60, https://doi.org/10.3390/futurepharmacol5040060.
45. Hara, C.d.C.P.; Honorio-Franca, A.C.; Fagundes, D.L.G.; Guimarães, P.C.L.; França, E.L. Melatonin Nanoparticles Adsorbed to Polyethylene Glycol Microspheres as Activators of Human Colostrum Macrophages. *J. Nanomater.* **2013**, *2013*, 973179, https://doi.org/10.1155/2013/973179.

Publisher's Note & Disclaimer

information before relying on it, and the publisher assumes no responsibility for any consequences arising from the use of materials contained in this publication.